Electronic Supplementary Information

Selenium-Containing Heterodimeric Crown Ether Acting as an Unconventional Multi-Responsive Amphiphile in water

Jie Shang,[a] Shuangran Li,[a] Tiezheng Pan,[a] Bo Li,[a] Qian Zhang,[a] Ping Lv[a], Zhiliyu Cui,[a] Yan Ge,*[a] Zhenhui Qi*[a]

[a]Sino-German Joint Research Lab for Space Biomaterials and Translational Technology, Synergetic Innovation Center of Biological Optoelectronics and Healthcare Engineering (BOHE) Shaanxi Provincial Synergistic Innovation Center for Flexible Electronics & Health Sciences (FEHS), School of Life Sciences, Northwestern Polytechnical University, Xi'an, Shaanxi 710072, P. R. China

Email: qi@nwpu.edu.cn; ge@nwpu.edu.cn

Table of Contents

1. General Methods and Materials

All reagents were commercially available and used without further purification. Compounds **3**, **4** were synthesized by the protocol developed in our group.[S1,S2] Milli-Q water was used in all measurements. Nuclear magnetic resonance (NMR) spectra were recorded with a Bruker Avance III-400 spectrophotometer, using the deuterated solvent as the lock and residual solvent or TMS as the internal reference. For the structural characterization of synthetic compounds, high-resolution mass spectrum (HR-MS) was performed using an electrospray ionization (ESI) interface on an Agilent LC/MSD TOF system. The transmittance experiments were measured at 700 nm using a ThermoFisher Evolution 260 Bio UV/Vis spectrometer with a temperature controllable system. The heating rate was adjusted at 1.0 °C min^{-1}. Fluorescence experiments were performed in 1.0 cm quartz cuvettes and recorded on an F-380 spectrofluorimeter (GANGDONG SCI. & TECH.) in the range of 250 to 760 nm at excitation wavelength 250 nm with 5 nm slit. TEM images were obtained with a FEI Talos F200X transmission electron microscope with an accelerating voltage of 300 kV. Droplets (~1 μL) of aqueous solution of sample compounds were placed on carbon film coated copper grids (Electron Microscopy China, Beijing, China). The grids were allowed to air-dry at least 40 min and were subsequently transferred into the microscope without use of a contrasting step. SEM images were obtained with a Verios G4. Dynamic light scattering (DLS) was carried out on a Malvern Nanosizer S instrument at room temperature. The conductivities of aqueous anion salt solutions were determined on a DDS-307A instrument.

2. Synthesis and Characterization of Compounds

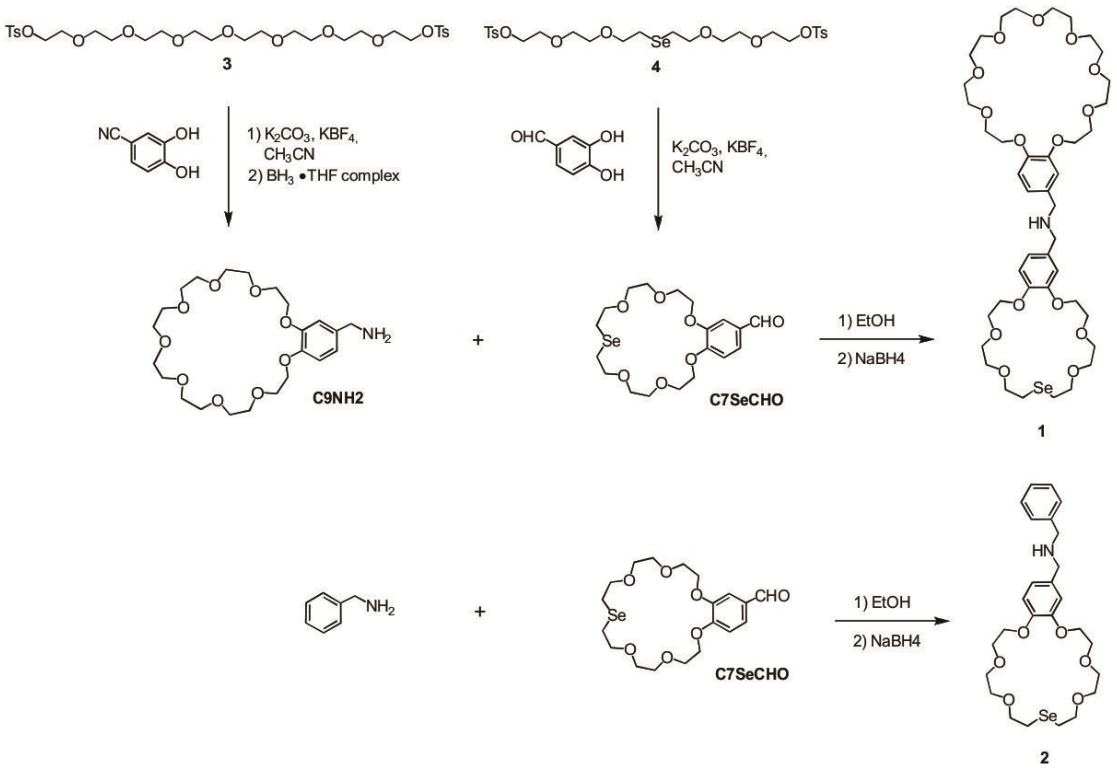

Scheme S1. The synthetic route of compounds **1** and **2**.

Preparation of Compound C9NH2

Step 1: While stirring vigorously under N_2 atmosphere, a suspension of K_2CO_3 (2.44 g, 17.68 mmol) and KBF_4 (4.45 g, 35.36 mmol) in anhydrous CH_3CN (150 mL) was heated to reflux. To the suspension, a solution of the compound **3** (2.00 g, 2.95 mmol) prepared according literature[S3] and 3,4-dihydroxybenzonitrile (0.40 g, 2.95 mmol) in CH_3CN (100 mL) was added dropwise. The resulting reaction mixture was stirred under reflux for 48 h at 75 °C. After cooling to r.t., the suspension was filtered and washed with CH_2Cl_2 (80 mL). The filtrate was concentrated in vacuo. Then the residue was dissolved in CH_2Cl_2 (100 ml) and washed by brine (100 ml). The organic phases were dried over anhydrous Na_2SO_4, and concentrated under reduced pressure to give the crude product, which was purified by silica gel column chromatography (CH_2Cl_2/MeOH, *v*/*v* 100:1 → 50/1 and EA/MeOH, *v*/*v* 100:1 → 40/1) to yield the cyano-substituted intermediate **C9** (1.12 g, 80.9%) as a yellow oil. ^{1}H NMR (400 MHz, $CDCl_3$) δ 7.25 (d, J = 1.9 Hz, 1H), 7.12 (d, J = 1.8 Hz, 1H), 6.91 (d, J = 8.4 Hz, 1H), 4.23 – 4.14 (m, 4H), 3.91 (dd, J = 9.2, 5.6 Hz, 4H), 3.79 – 3.75 (m, 4H), 3.70 – 3.65 (m, 20H); ^{13}C NMR (100 MHz, $CDCl_3$) δ = 153.08, 149.05, 126.90,

119.36, 116.94, 113.40, 104.18, 71.26, 71.24, 70.91, 70.85, 69.73, 69.58, 69.18; HR-MS (ESI) *m/z* ($M+Na^+$) calcd. for $C_{23}H_{35}NO_9Na^+$: 492.2210, Found: 492.2211.

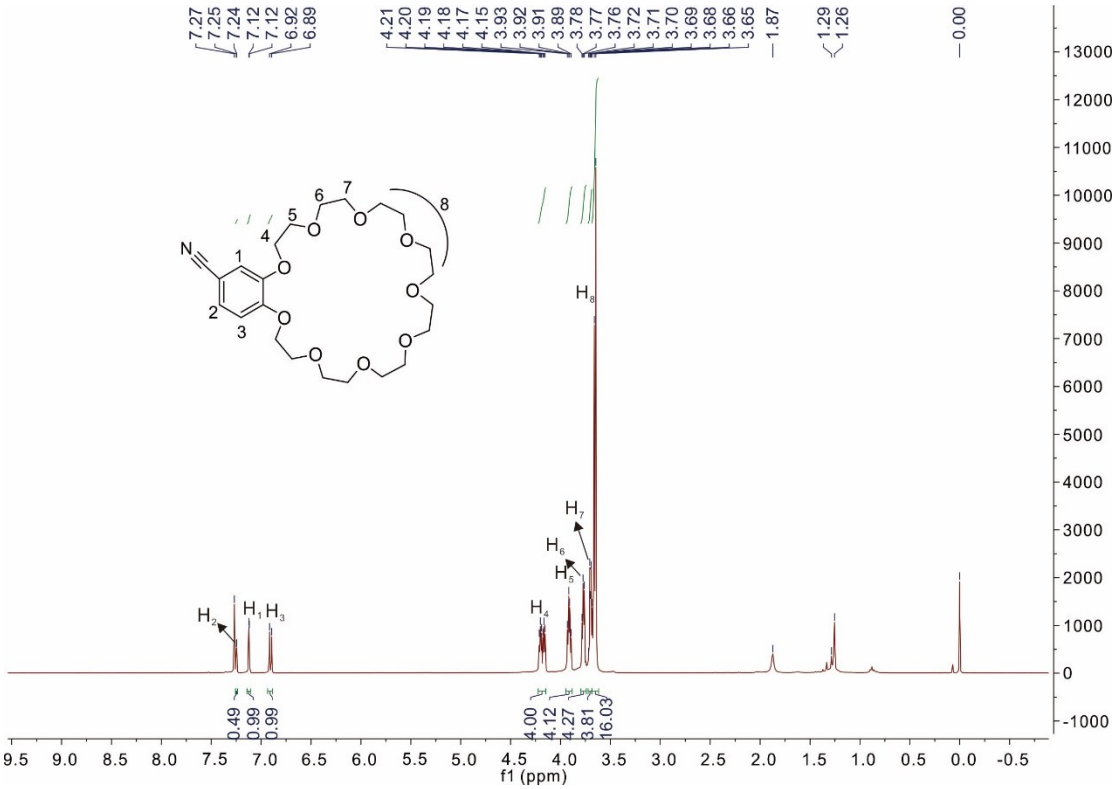

Figure S1. ^{1}H NMR spectrum (400 MHz, $CDCl_3$, 298K) of intermediate **C9CN**.

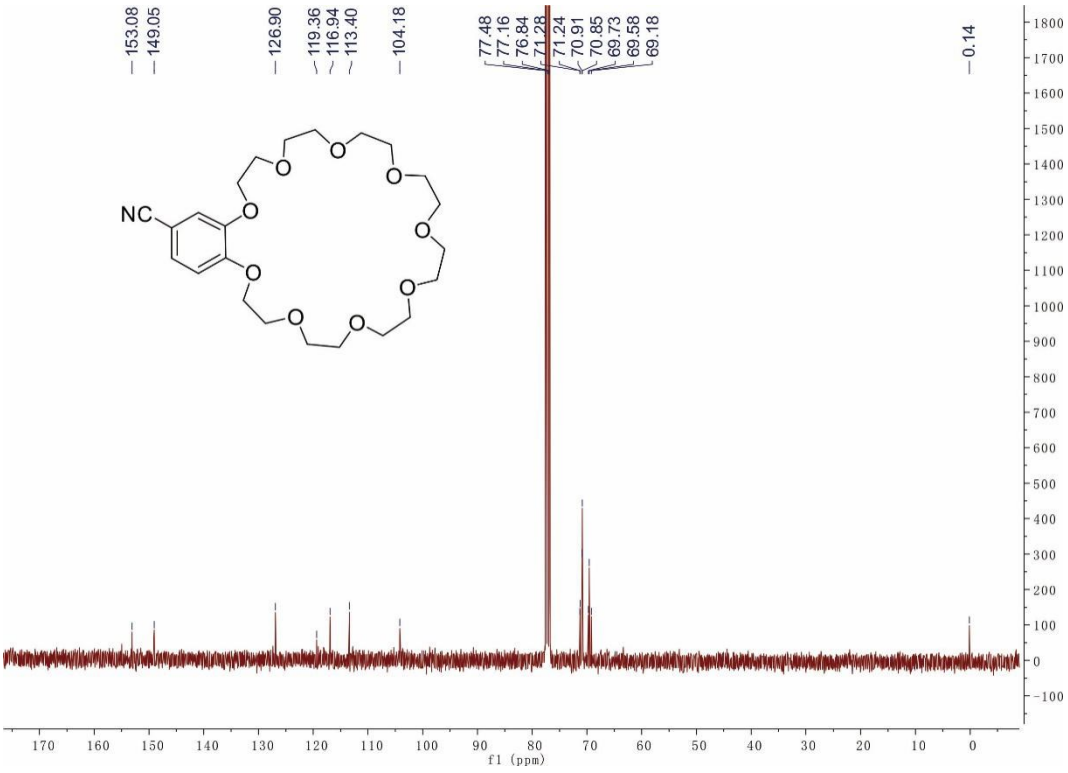

Figure S2. ^{13}C NMR spectrum (100 MHz, $CDCl_3$, 298K) of intermediate **C9CN**.

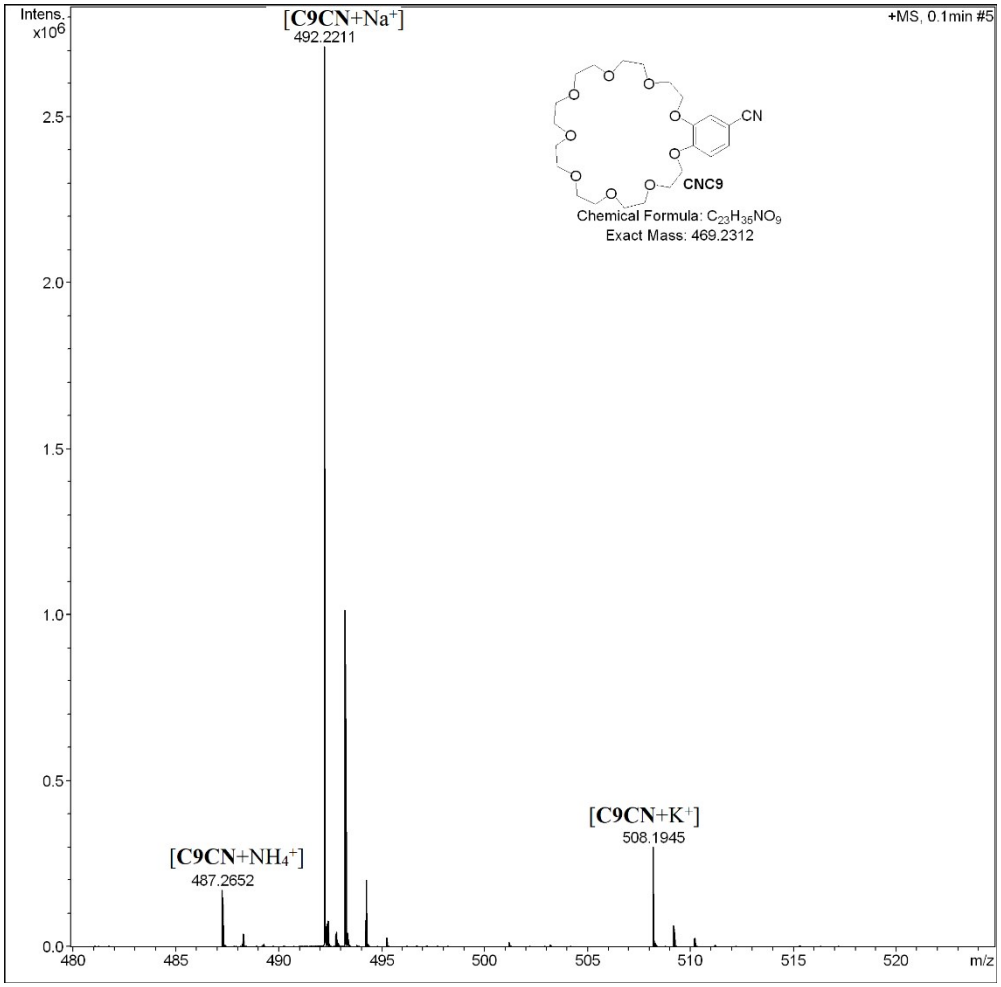

Figure S3. HR-MS characterization of intermediate **C9CN**.

Step 2: The obtained intermediate **C9CN** (1.50 g, 3.19 mmol) was further dissolved in dissolved in dry THF (50 mL), which was added by a solution of borane-tetrahydrofuran complex (32 mL of 1 M BH_3•THF, 32.0 mmol) in dry THF (75 mL) at 0 ˚C. The solution was stirred for 30 min at 0 °C, then it was heated to reflux for 20 h. After refluxing, the reaction mixture was cooled to 0 °C, and hydrochloric acid (1.6 mL, 37% in water) dissolved in methanol (37 mL) was added dropwise (be careful: hydrogen gas evolution), and the reaction mixture was stirred for additional 1 h and subsequently evaporated to dryness under reduced pressure. The residue was dissolved in methanol (80 mL) and the solution was concentrated to dryness, then repeat this procedure twice. The viscous liquid was dissolved in sodium hydroxide solution (150 mL, 1 M), and the aqueous was extracted by dichloromethane 100 mL x 3. The combined organic layers were dried over anhydrous Na_2SO_4 and filtered. The filtrate was concentrated under reduced pressure. Then 0.1 M HCl was added into the residue dissolved in H_2O (8 mL) to adjust the pH to 1~2. The liquid mixture was washed by n-heptane 8 mL x 8, and the aqueous was adjusted pH to 11~12 by sodium hydroxide solution (1 M in water). Then the water layer was extracted by dichloromethane

40 mL x 3. The combined organic layers were dried over anhydrous Na_2SO_4, and concentrated under reduced pressure to yield pure compound **C9NH$_2$** (1.44 g, 95.0%) as a yellow oil. ^{1}H NMR (400 MHz, $CDCl_3$) δ = 6.88-6.82 (m, 3H), 4.22 – 4.11 (m, 4H), 3.90 – 3.87 (m, 4H), 3.79 – 3.78 (m, 6H), 3.73 – 3.62 (m, 20H).

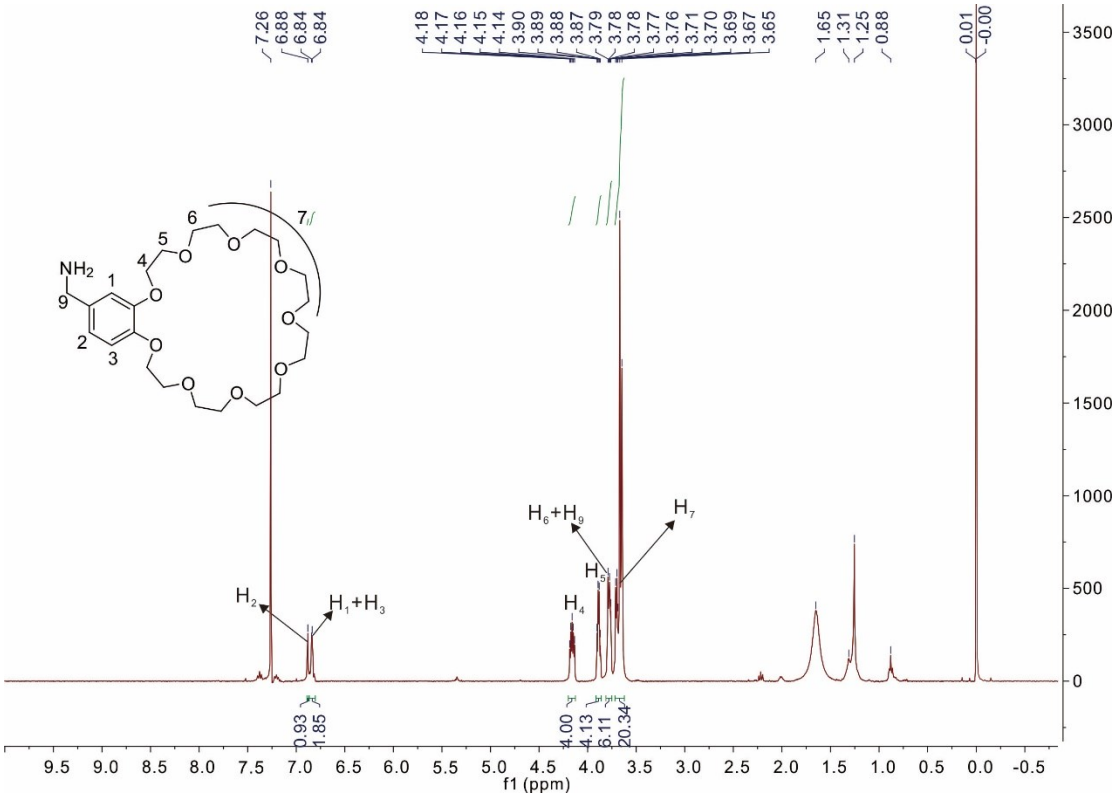

Figure S4. ^{1}H NMR spectrum (400 MHz, $CDCl_3$, 298K) of **C9NH2**.

Preparation of Compound C7SeCHO

K_2CO_3 (5.06 g.36.6 mmol) and KBF_4 (4.62 g, 36.6 mmol) was suspended in CH_3CN (300 mL) degassed by nitrogen and was heated to 75~80 ˚C. Compound **4** (8.0 g, 12.2 mmol) prepared according literature[S2] and 3,4-dihydroxybenzaldehyde (1.69 g, 12.2 mmol) dissolved in CH_3CN (100 mL) and was added dropwise during 5 h. After addition, the mixture was stirred at 80 ˚C overnight. The reaction was cooled to room temperature and was filtered. The cake was washed by CH_2Cl_2 50 mL twice. The filtrate was concentrated under reduced pressure. The residue was resolved in 100 mL CH_2Cl_2, then the solution was washed by brine 50 mL. After drying the organic layer over Na_2SO_4, solvents were removed, the residue was purified by silicon column with CH_2Cl_2/MeOH (500/1~500/10, *v*/*v*) to yield pure compound **C7SeCHO** (3.7 g, 68%) as a yellow oil. ^{1}H NMR (400 MHz, $CDCl_3$) δ = 9.84 (s, 1H), 7.48 – 7.39 (m, 2H), 6.97 (d, *J* = 8.2, 1H), 4.26 – 4.21 (m, 4H), 3.97 – 3.92 (m, 4H), 3.82-3.76 (m, 8H), 3.68 – 3.66 (m, 4H), 2.83 (td, *J*

= 6.4, 1.8, 4H); ^{13}C NMR (100 MHz, CDCl3) δ = 191.03, 154.52, 149.35, 130.38, 126.97, 112.54, 111.84, 72.58, 72.52, 71.19, 71.13, 70.51, 70.49, 69.76, 69.62, 69.13 (s), 29.82, 23.17, 23.15; HR-MS (ESI) *m/z* (M+Na$^+$) *calcd*. for $C_{19}H_{28}O_7SeNa^+$: 471.0898, *Found*: 471.0902.

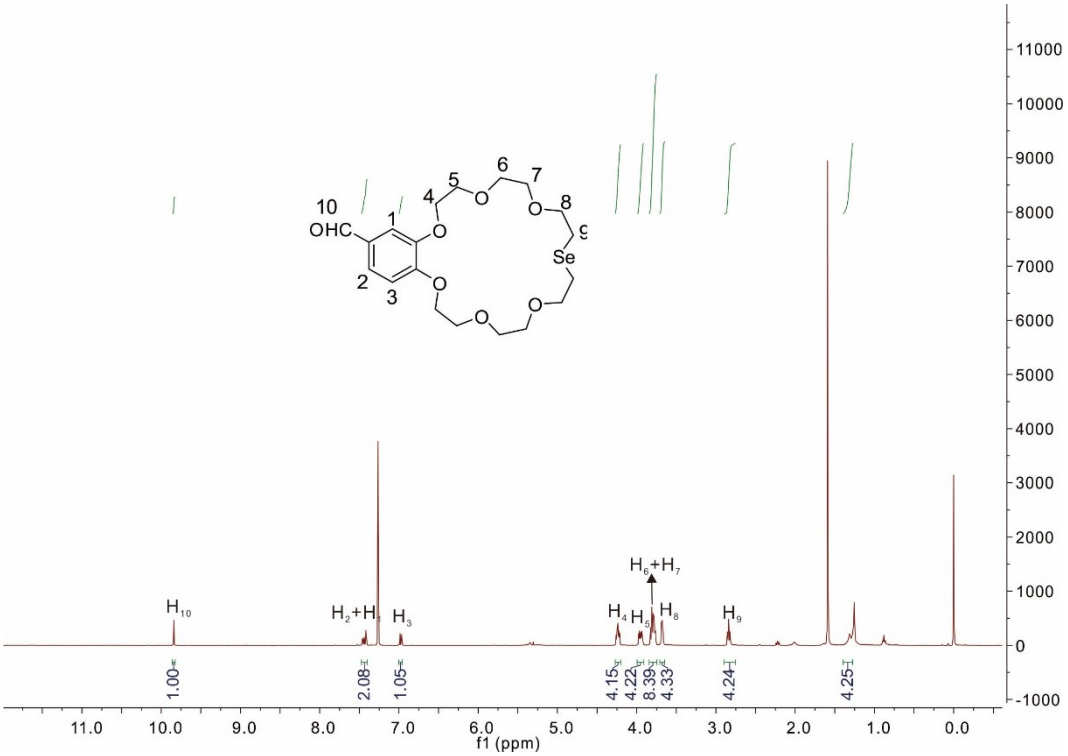

Figure S5. ^{1}H NMR spectrum (400 MHz, $CDCl_3$, 298K) of **C7SeCHO**.

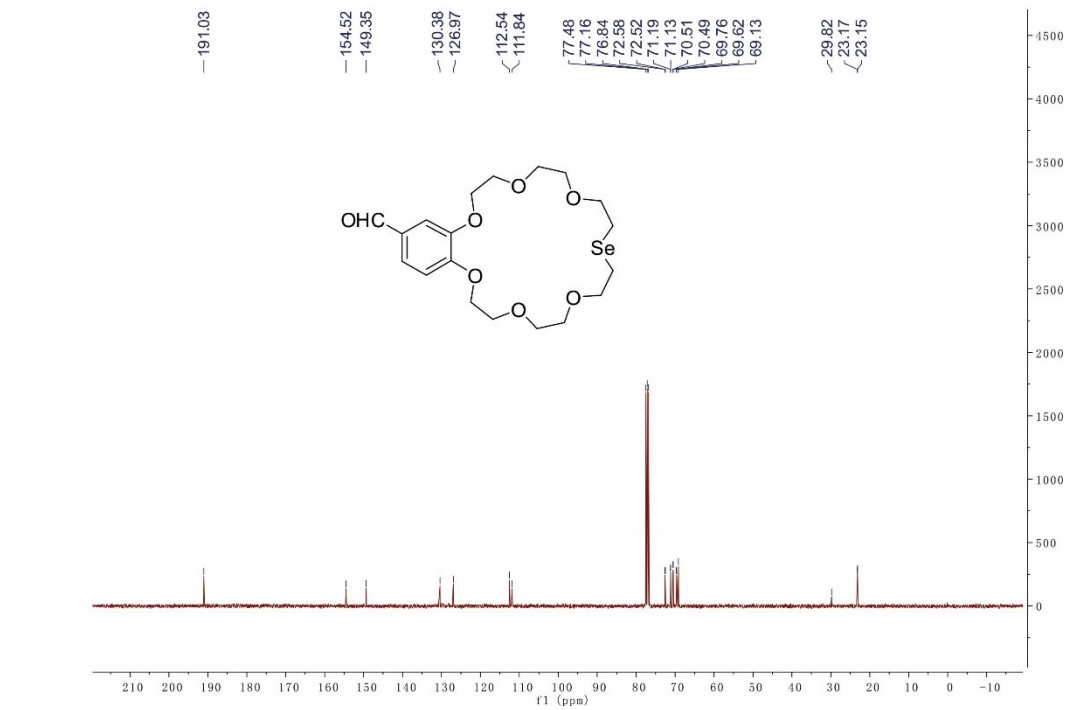

Figure S6. ^{1}C NMR spectrum (100 MHz, $CDCl_3$, 298K) of **C7SeCHO**.

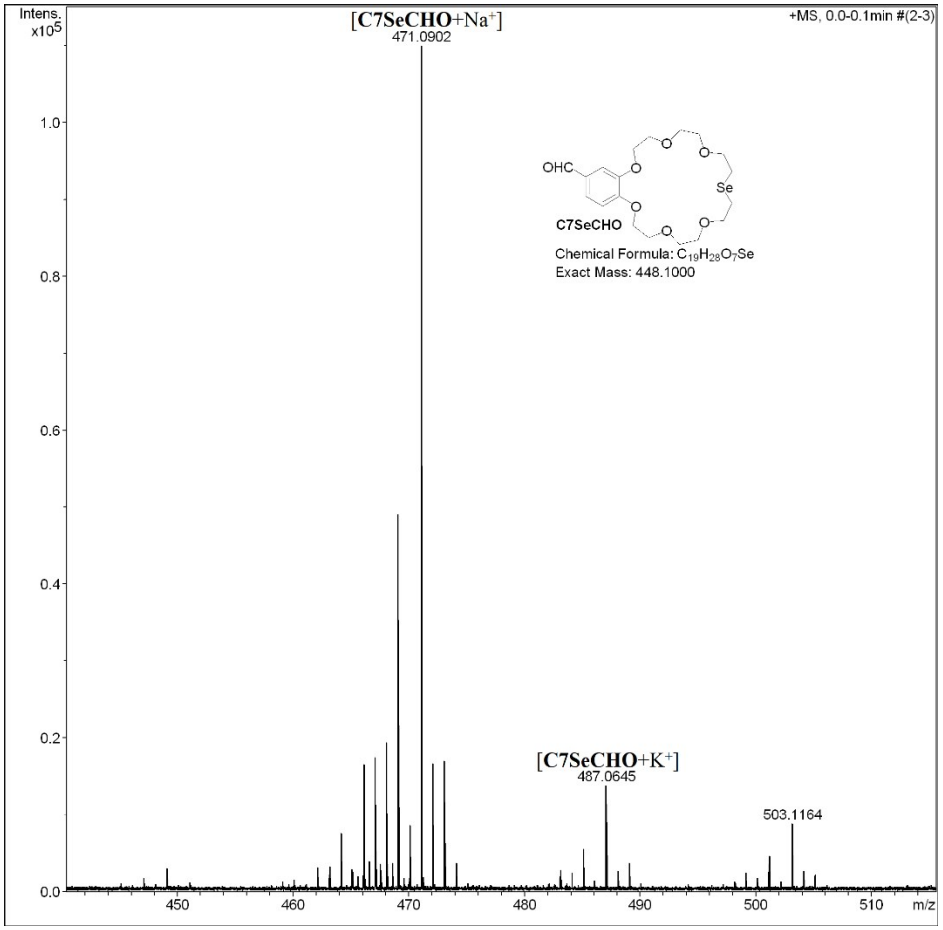

Figure S7. HR-MS characterization of **C7SeCHO**.

Preparation of Compound 1

Compound **C9NH2** (100 mg, 0.21 mmol) and compound **C7SeCHO** (99.3 mg, 0.22 mmol.) were dissolved in anhydrous EtOH (10 mL) under N_2 atmosphere and Na_2SO_4 (0.5 g) was added. The mixture was heated to reflux and stirred for 36 h. After TLC showed compound **C9NH2** was consumed completely (MeOH/DCM = 15/1, *v*/*v*), the solution was cooled to room temperature. $NaBH_4$ (24 mg, 0.63 mmol) was added and the mixture was stirred for another 24 h at 25 ℃ under N_2 protection. Solvent was removed under reduced pressure and the residue was suspended in 50 ml DCM. To the mixture 30 brine was added, it was stirred for 0.5 h. Organic layer was dried over Na_2SO_4. Solvent was removed under reduced pressure and the residue was purified by prepared silicon plate with MeOH/DCM = 1/20 (*v*/*v*) as eluent. Product was washed from silicon by NH_4OH/MeOH/DCM = 2/10/100 (*v*/*v*/*v*). Product (110 mg) was obtained as a slight yellow oil (yield: 58%). ^{1}H NMR (400 MHz, $CDCl_3$) δ = 6.91 (s, 2H), 6.84 (d, J = 1.7, 4H), 4.19 – 4.14 (m, 8H), 3.91 – 3.86 (m, 8H), 3.82 – 3.76 (m, 12H), 3.70 – 3.65 (m, 28H), 2.84 (t, J = 6.5, 4H); ^{13}C

NMR (101 MHz, $CDCl_3$) δ = 148.98, 148.94, 147.96, 147.95, 133.36, 133.25, 121.16, 121.09, 114.55, 114.47, 114.39, 114.27, 72.46, 74.42, 70.93, 70.88, 70.71, 70.67, 70.42, 70.38, 69.92, 69.90, 69.84, 52.60, 29.72, 22.95; HR-MS (ESI) *m/z* ($M+H^+$) *calcd*. for $C_{42}H_{67}NO_{15}SeH^+$: 906.3676. *Found*: 906.3744.

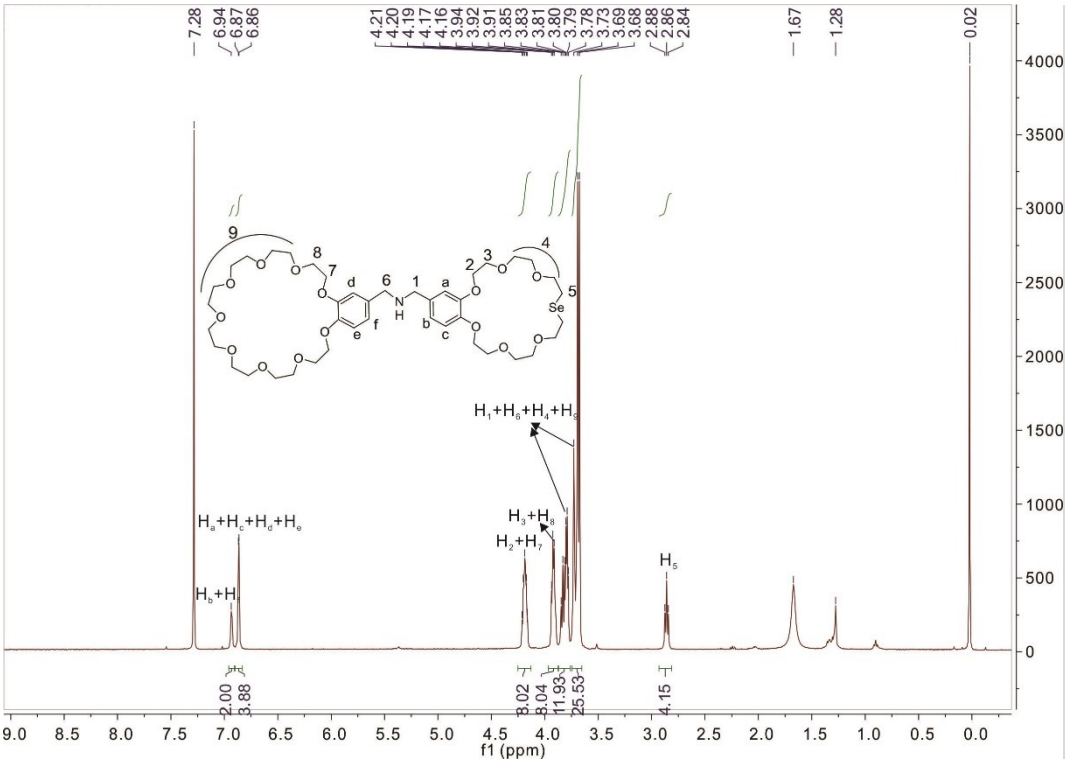

Figure S8. ^{1}H NMR spectrum (400MHz, $CDCl_3$, 298K) of **1**.

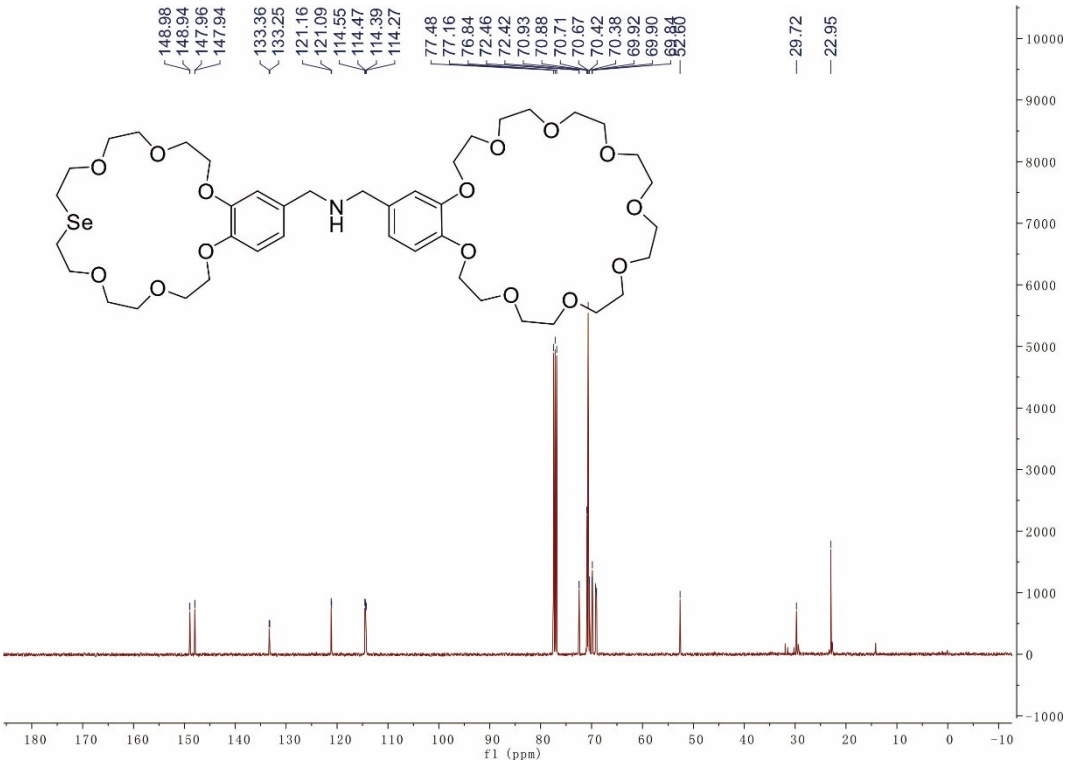

Figure S9. ^{13}C NMR spectrum (100 MHz, $CDCl_3$, 298K) of **1**.

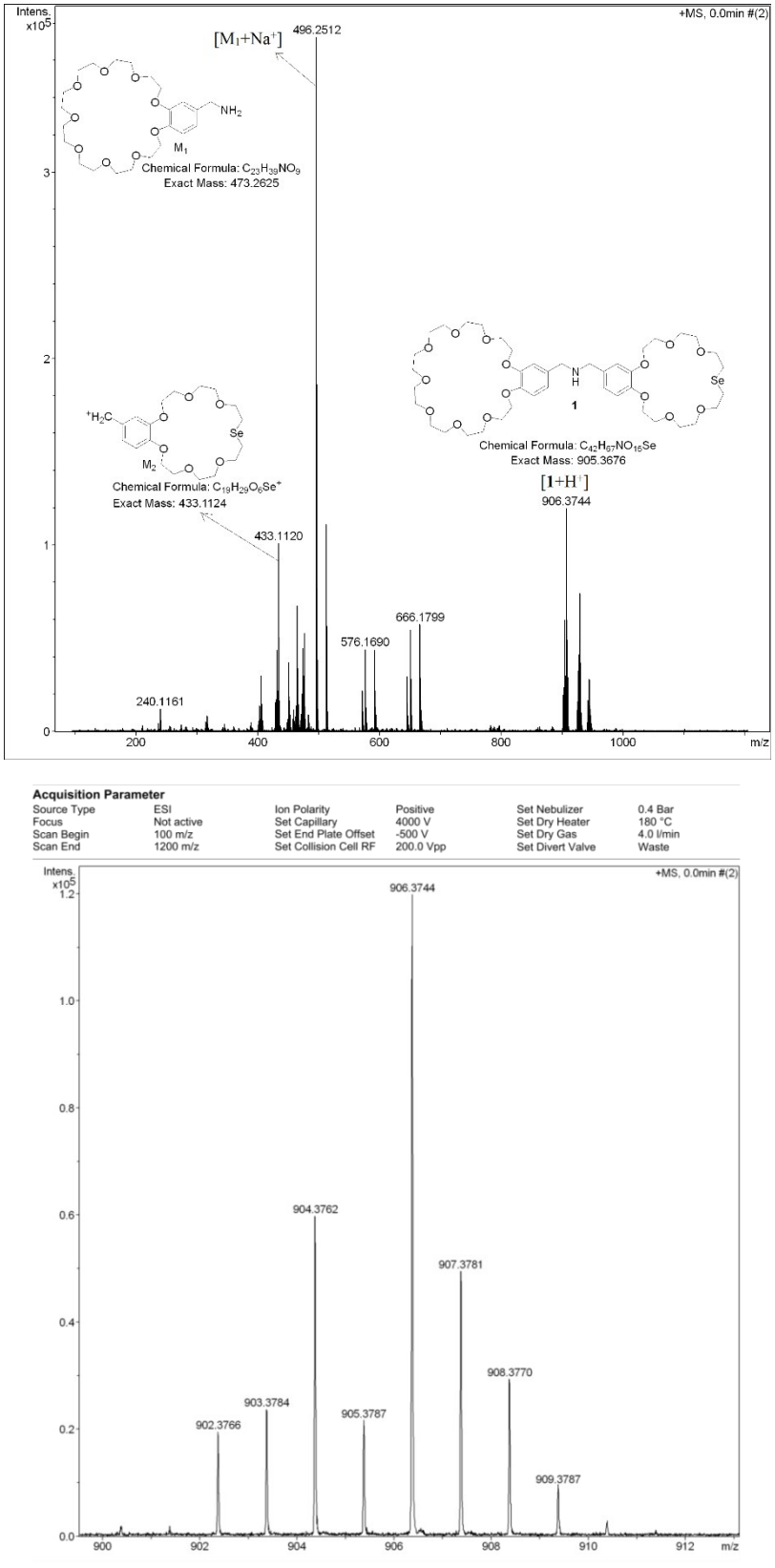

Figure S10. HR-MS characterization of **1**. The full spectrum (top) and isotopic pattern (bottom) of the target compound. The peak at *m/z* 906 shows characteristic isotopic pattern of selenium, indicating the successful incorporation of selenium atom in amphiphile **1**.

Preparation of Compound 2

Compound **2** was synthesized by the similar protocol employed for **1**, except using benzyleamine. Product (150 mg) was obtained as a slight yellow oil (yield: 62%). ^{1}H NMR (400 MHz, $CDCl_3$) δ = 7.33 (d, J = 4.3 Hz, 4H), 7.26 – 7.23 (m, 1H), 6.92 (s, 1H), 6.85 (s, 2H), 4.23 – 4.11 (m, 4H), 3.96 – 3.86 (m, 4H), 3.87 – 3.74 (m, 10H), 3.73 (s, 2H), 3.68 – 3.66 (m, 4H), 2.84 (t, J = 6.5 Hz, 4H). ^{13}C NMR (100 MHz, $CDCl_3$) δ = 149.22, 148.13, 140.35, 133.94, 128.51, 128.28, 127.06, 121.22, 114.93, 72.55, 71.04 , 70.52, 70.06, 69.38, 53.55, 53.17, 52.88, 23.08.. HR-MS (ESI) *m/z* ($M+H^+$) *calcd*. for $C_{26}H_{37}NO_6SeH^+$: 540.1684, *Found*: 540.1863.

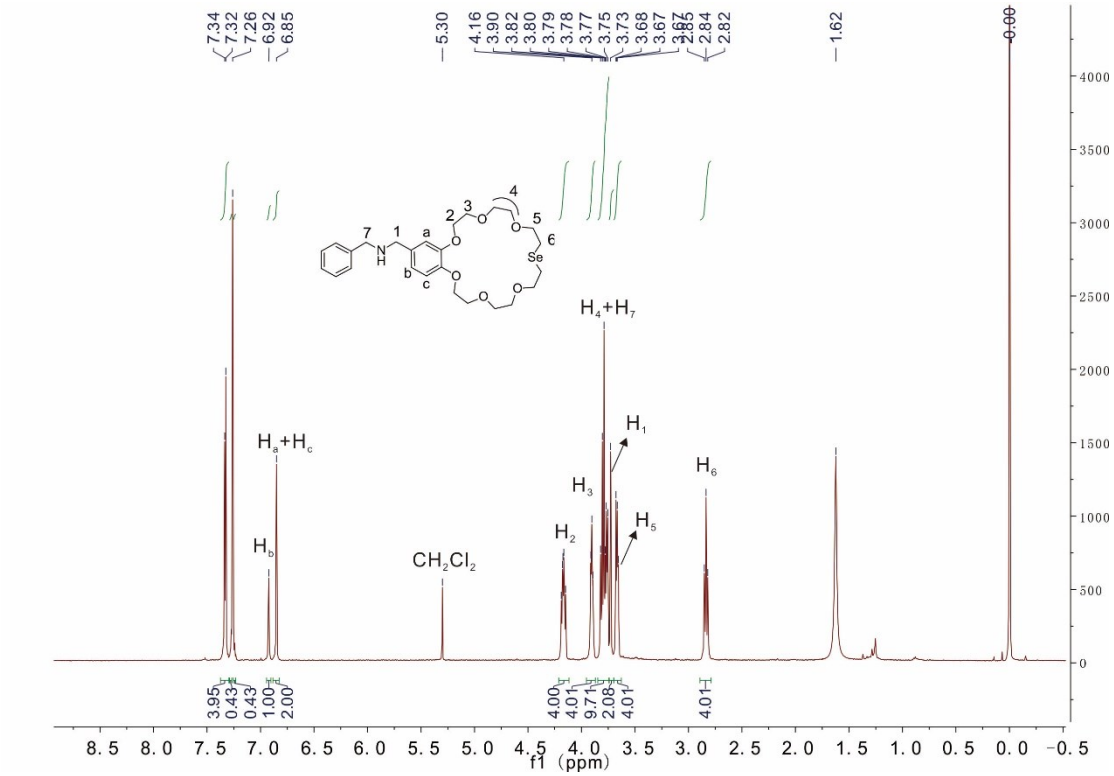

Figure S11 ^{1}H NMR spectrum (400MHz, $CDCl_3$, 298K) of **2**.

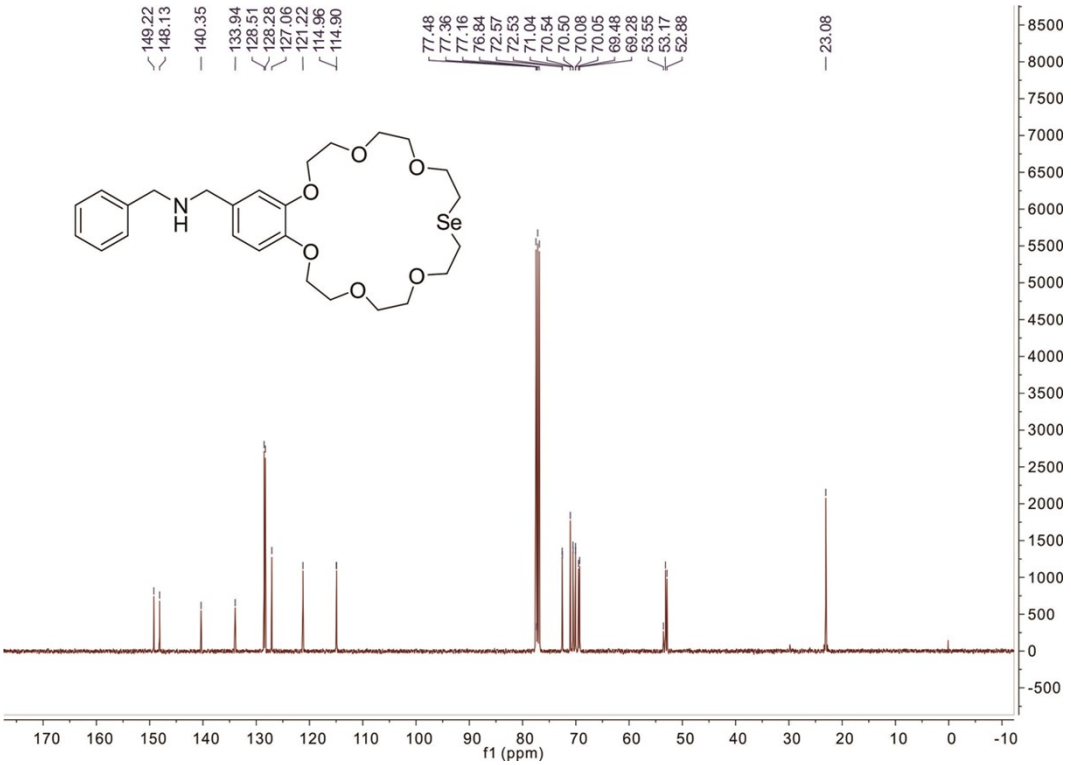

Figure S12. ^{13}C NMR spectrum (100 MHz, $CDCl_3$, 298K) of **2**.

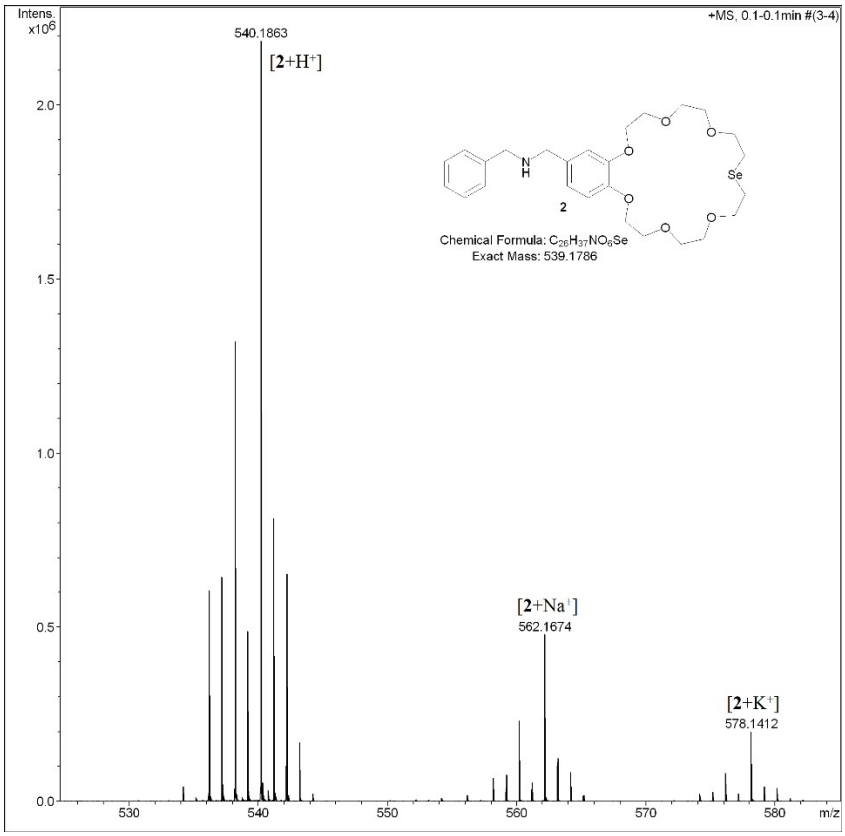

Figure S13. HR-MS characterization of **2**.

3. The solubility test of 1 in water

Figure S14. Image of compound **1** in water (12 mM) after vigorous shaking.

4. Self-Assembly Behaviors of Amphiphile 1 in Water

4.1 UV/Vis Investigation

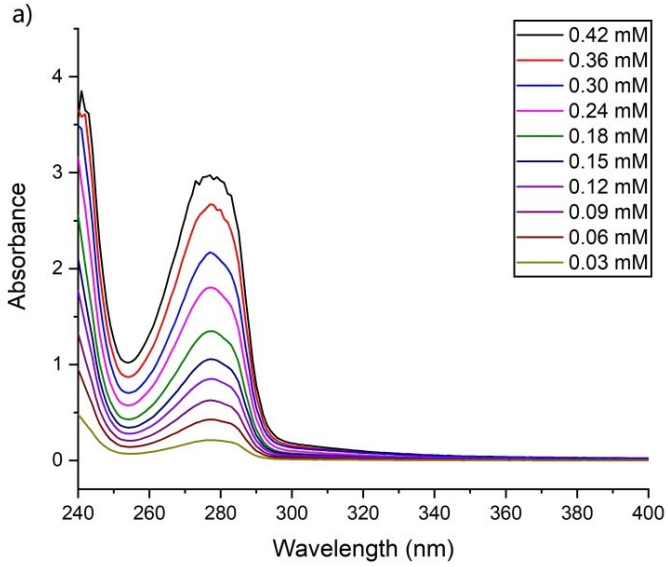

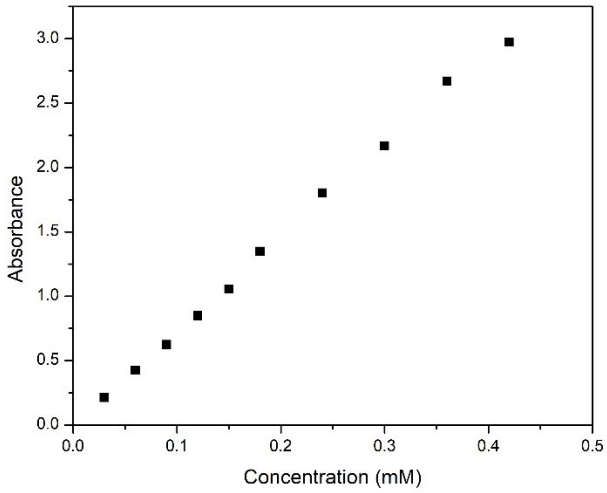

Figure S15. UV/Vis spectra of crown amphiphile **1** in water with different concentration in aqueous, there is a constant increase of the absorption as the concentration of **1** increase.

4.2 ^{1}H NMR investigation

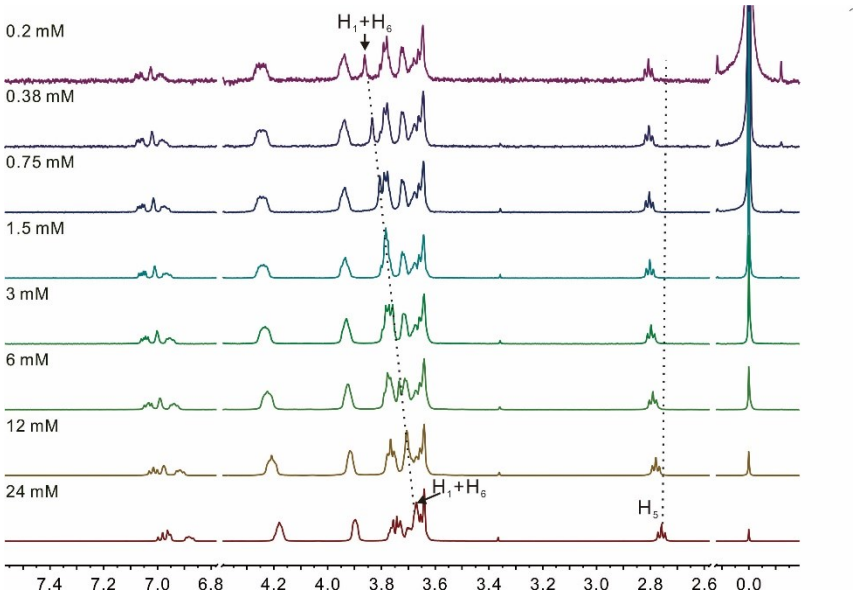

Fig. S16. Changes in ^{1}H NMR spectral of compound **1** with different concentration (D_2O, 500 MHz, 293 K, d_4-trimethylsilyspropionic acid sodium salt as internal standard). The proton signal shifted downfield with concentration decreased suggested compound **1** was aggregates at 0.2 mM in aqueous.

4.3 Fluorescence Investigation

a)

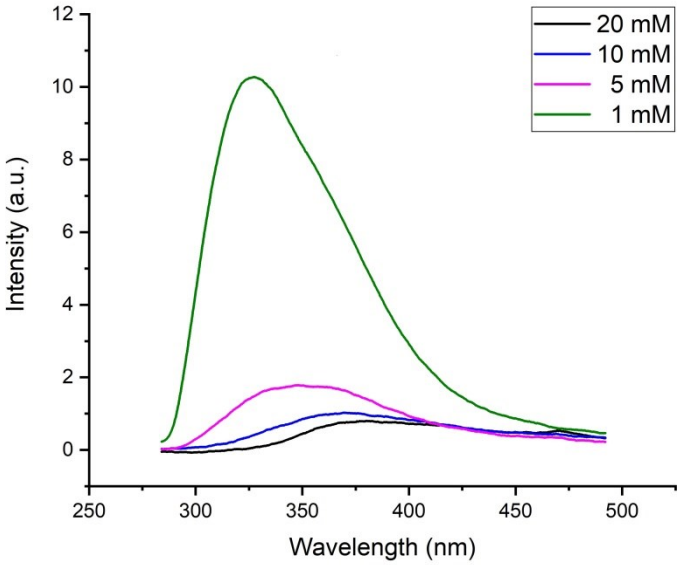

b)

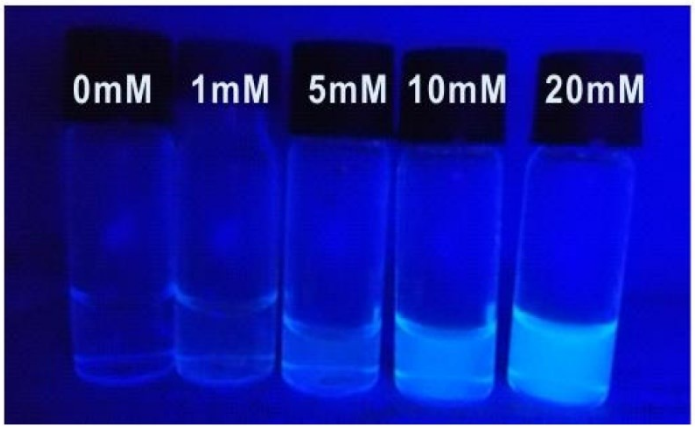

Figure S17. a) Fluorescence intensity of aqueous solution of **1** with different concentrations (1, 5, 10, 20 mM) obtained under excitation wavelength of 250 nm. b) Photographs of aqueous solution of **1** with different concentration (0, 1, 5, 10, 20 mM) under the irradiation of UV light at a wavelength of 365 nm.

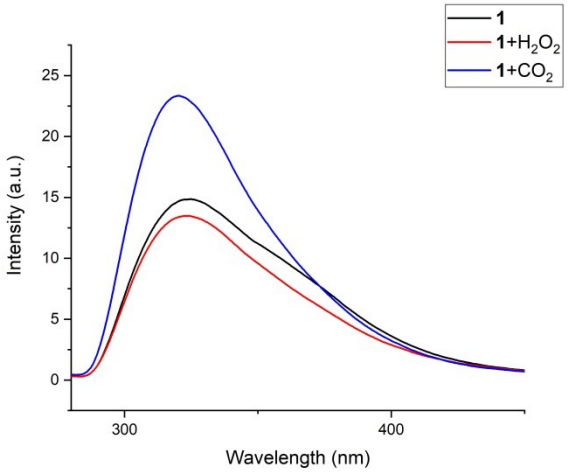

Figure S18. Fluorescence spectra upon addition of H_2O_2 and CO_2 to the aqueous solution of **1** at 1 mM. For oxidation, H_2O_2 (3 eq.) was added to the aqueous of **1**, The reason for fluorescence band slightly red shifted and the intensity of fluorescence decreased were considered compound **1** was oxidized to another compound and became needle-like shape. After bubbling CO_2 to the solution of **1**, the fluorescence band blue shifted and the intensity of fluorescence increased owing to the aggregates of **1** expanded by interaction with CO_2.

4.4 TEM Investigation

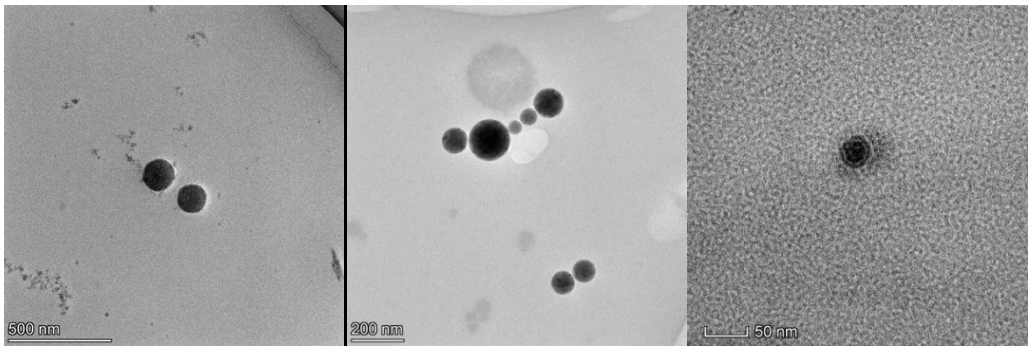

Figure S19. TEM images of the aggregate formed from **1** in water.

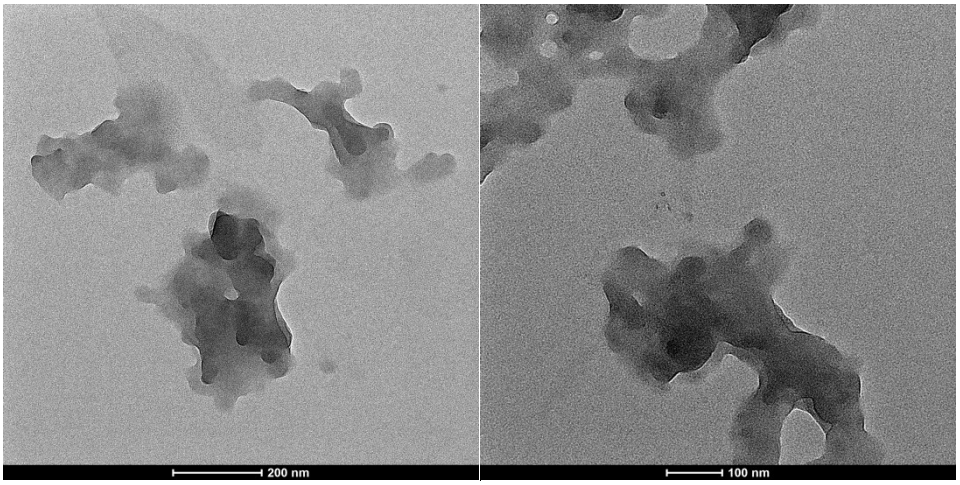

Figure S20. TEM images of the aggregate formed from **1** with DOX loading in water.

4.5 SEM Investigation

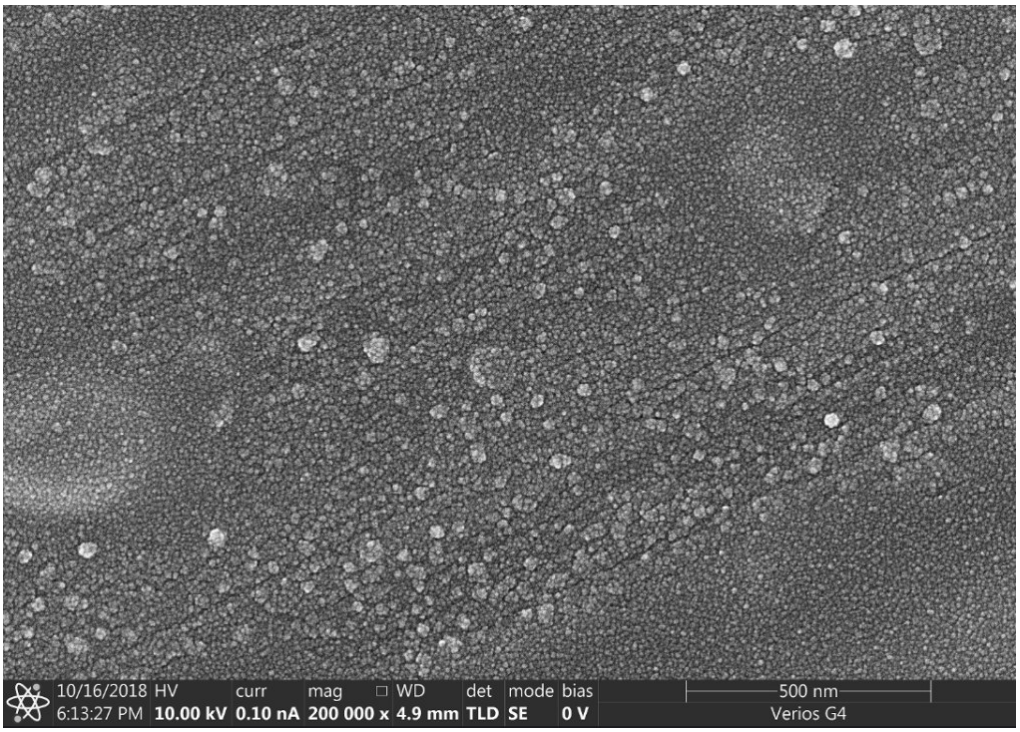

Figure S21. SEM images of the aggregate formed from **1** in water.

4.6 Small-Angle XRD Investigation

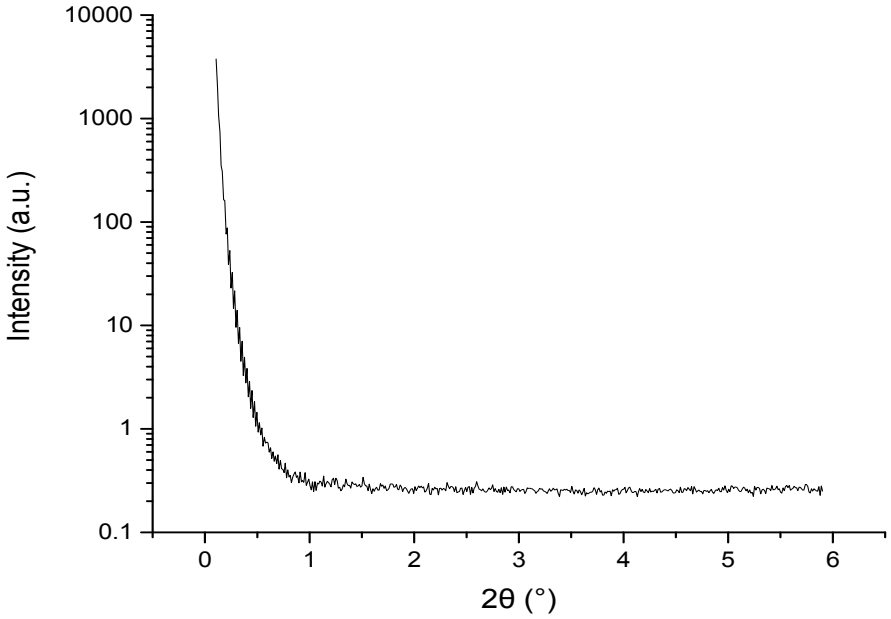

Figure S22. Small-angle X-ray scattering (SAXS) scan of **1** in water. $2d\text{Sin}\theta = \lambda = 0.1541$ nm, and $2\theta = 2.25^{\circ}$.[S4]

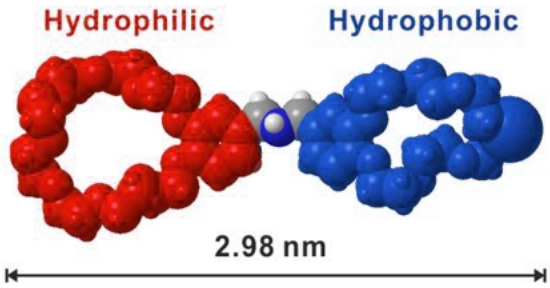

Figure S23. The simulated molecular length of amphiphile **1** is ~2.98 nm.

4.7 Determination of Critical Micelle Concentration

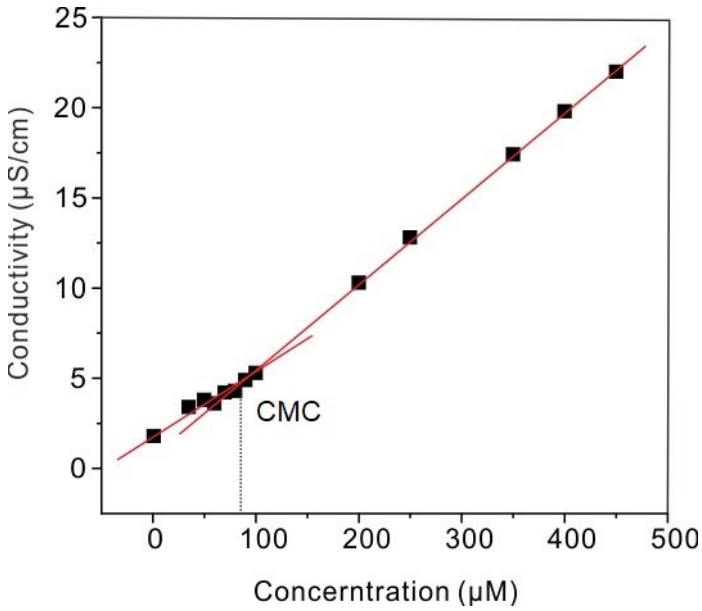

Figure S24. The concentration-dependent conductivity of **1** in water. The critical micelle concentration (CMC) was determined to be $(8.5 \pm 1)\times10^{-5}$ M.

4.8 2D NOESY Investigation

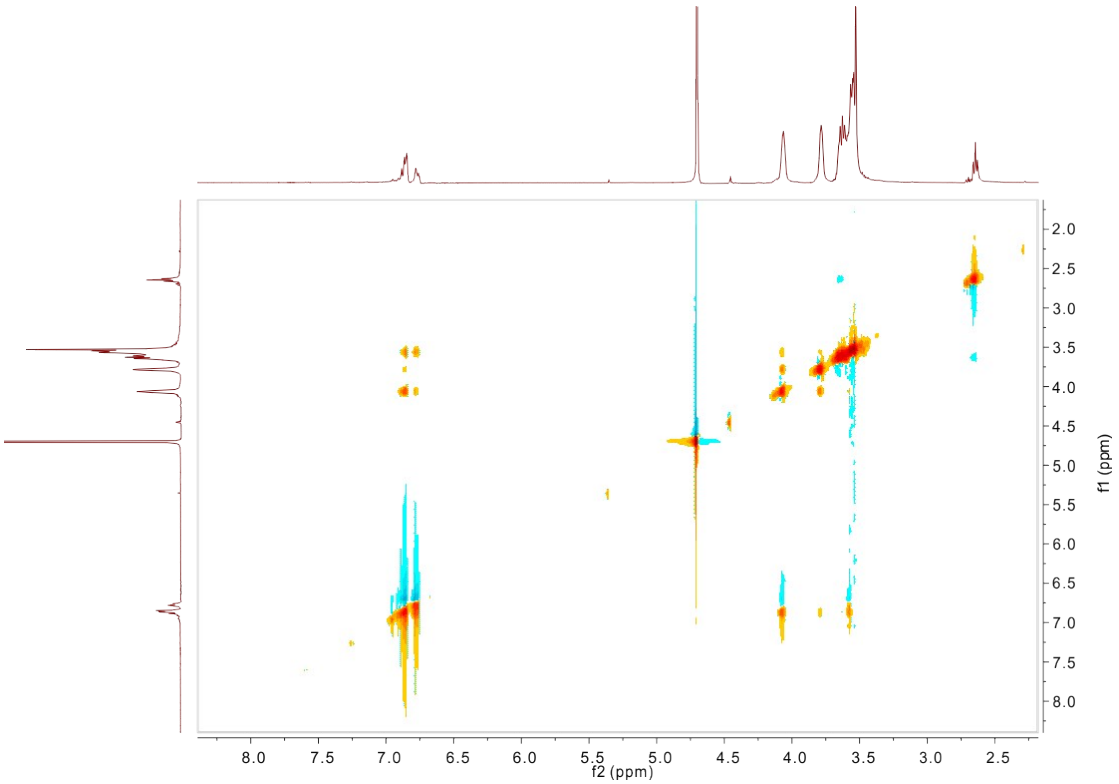

Figure S25. 2D NOESY spectrum (500 MHz, D_2O, 293 K) of **1** (12.0 mM).

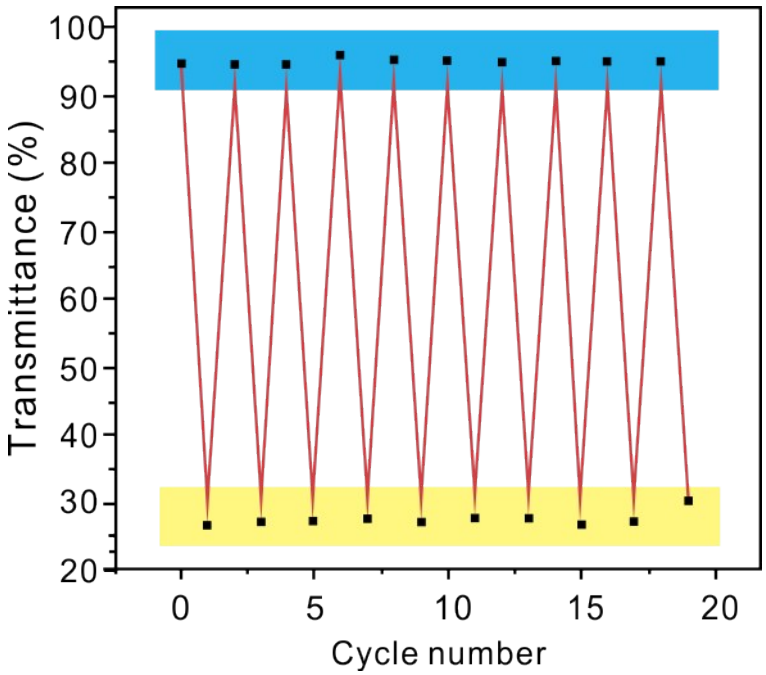

Figure S26. Changes in transmittance of **1** (12.0 mm) when cycling between 25 and 65 °C.

5. The solubility test of 2 in water

Figure 27. The photograph of **2** (2.8 mg) is insoluble in water (0.5 mL) **2** evidencing the strong hydration role of **C9** moiety.

6. Redox-responsive Behaviors of 1 in water

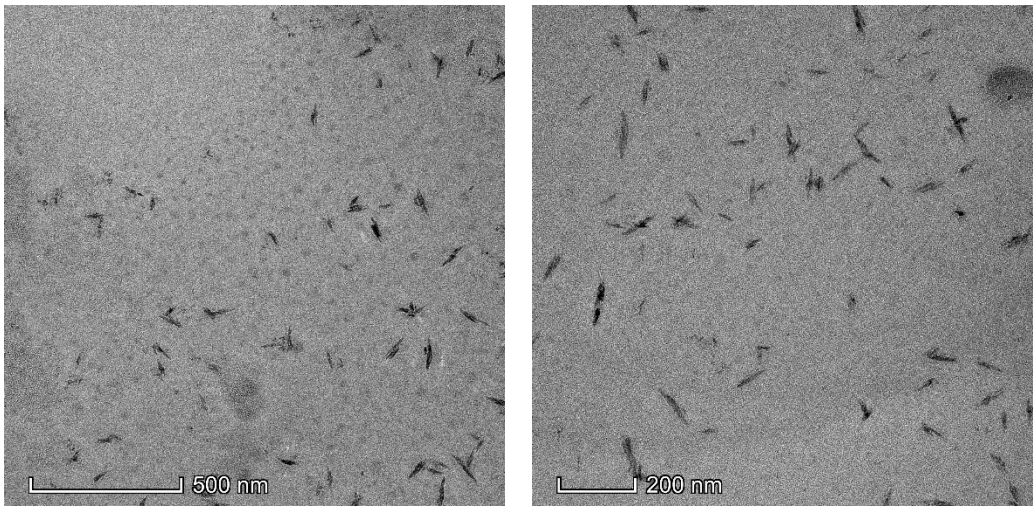

Figure S28. TEM images of **1** after oxidation. For oxidation, H_2O_2(3 eq.) was added to the aqueous of **1** (12 mM).

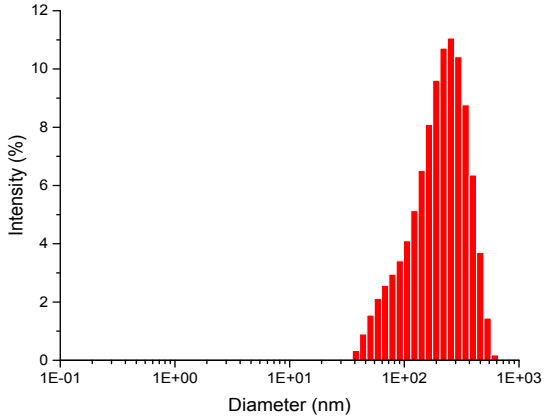

Figure S29. DLS of a solution of **1** (1 mM) in water after added H_2O_2 (3.0 eq.), the average diameter is 228.2 nm.

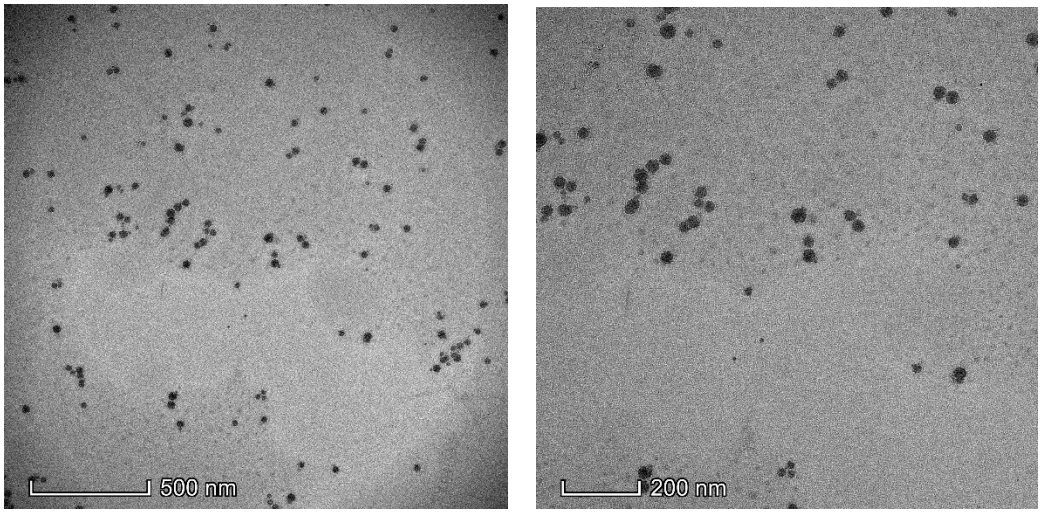

Figure S30. TEM images of **1** after the oxidation and then reduction. After **1** (12 mM) in water was oxidized by H_2O_2 (3.0 eq.), Vc (9 eq.) was added to the solution.

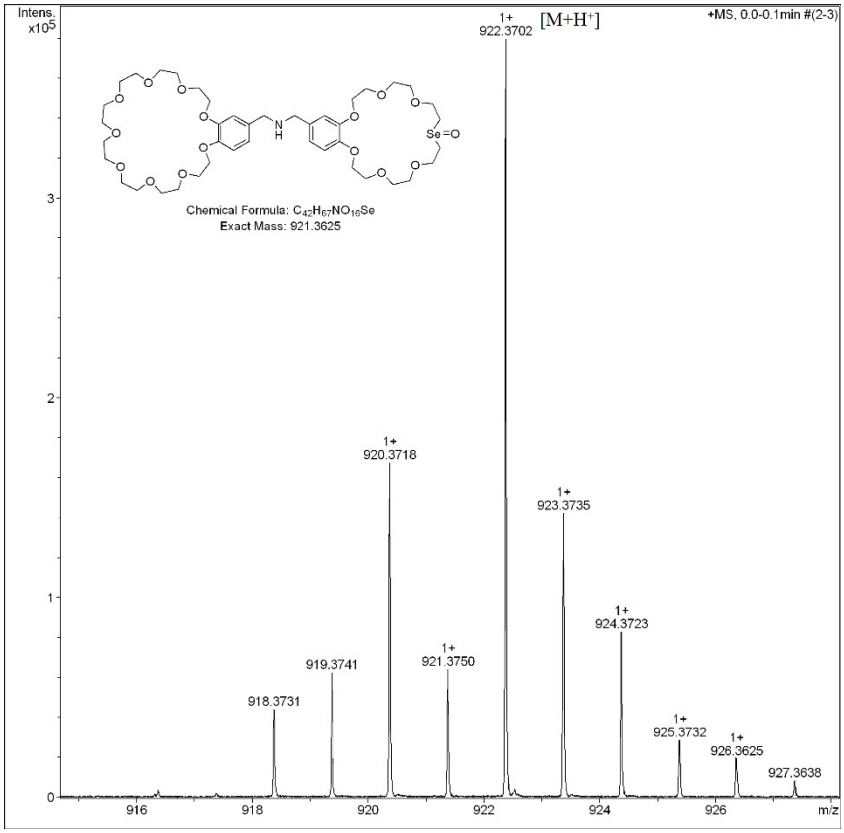

Figure S31. HR-MS characterization of **1** after oxidized by H_2O_2 in which the selenide is oxidized into the selenoxide.

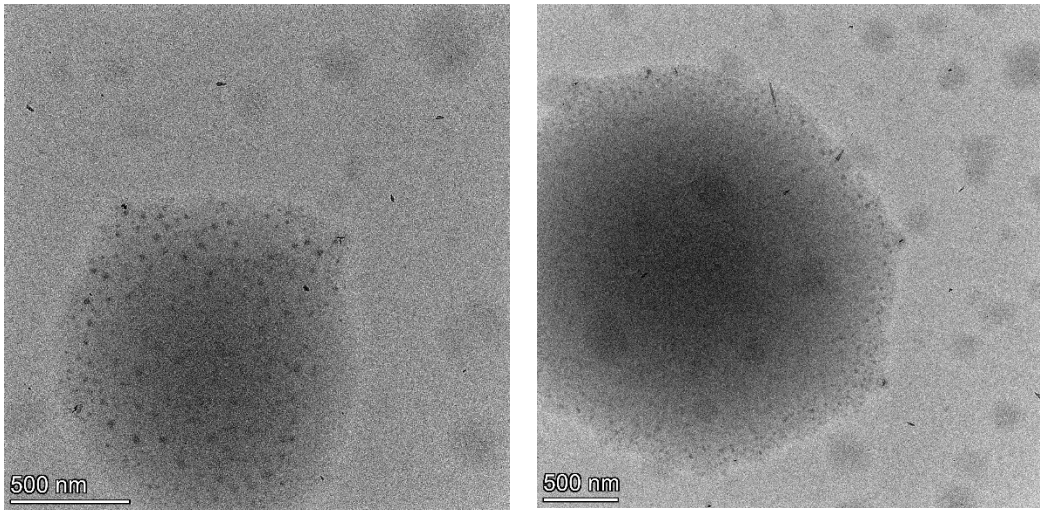

Figure S32. TEM images of aqueous solution of **1** (12 mM) after bubbling CO_2 (10 min)

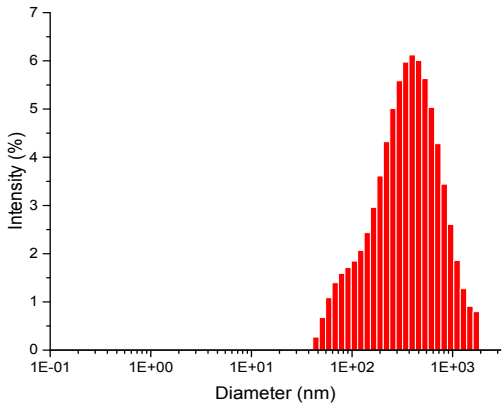

Figure S33. DLS of a solution of **1** (1 mM) in water after bubbled with CO_2, the average diameter is 367.5 nm.

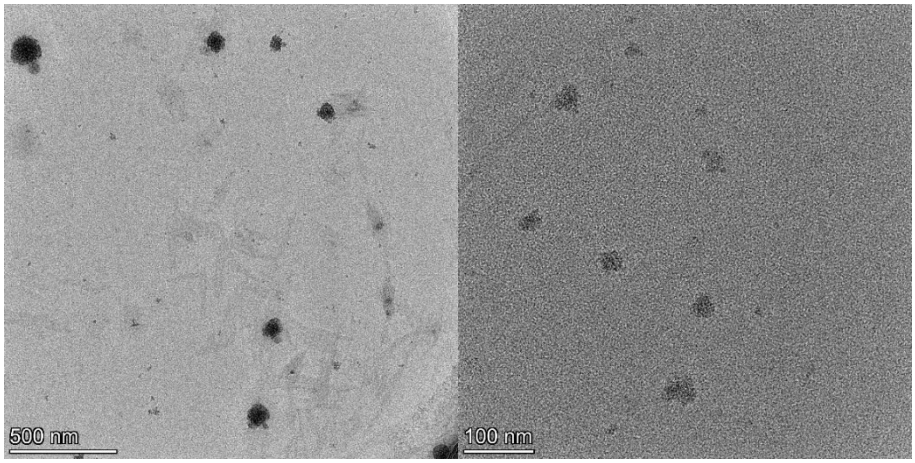

Figure S34. TEM images of aqueous solution of **1** (12 mM) after bubbling CO_2 (10 min), then bubbling Ar (20 min).

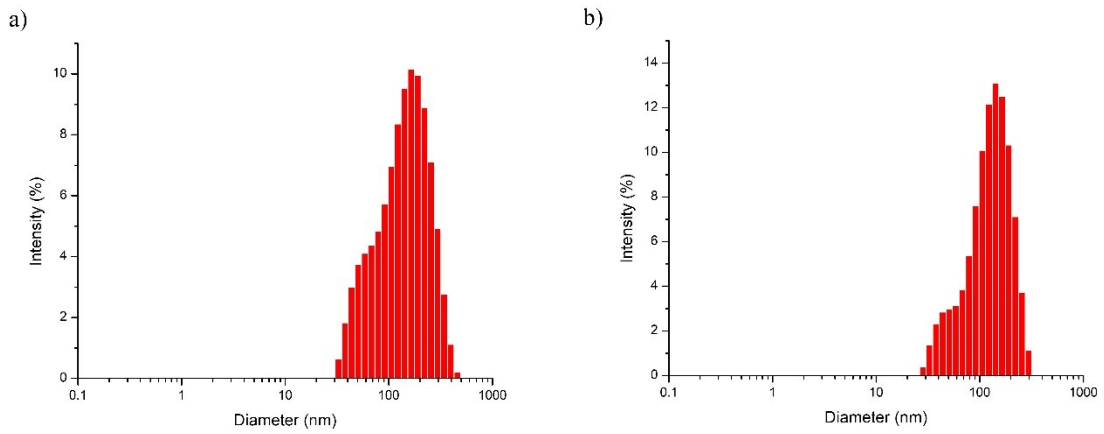

Figure S35. DLS of a solution of **1** (1 mM) in water a) after the oxidation by H_2O_2 and then reduction by Vc, the average diameter is 127.6 nm; b) bubbling CO_2, then bubbling Ar, the average diameter is 124.9 nm. These results further suggested that the vesicles based on **1** are responsive to H_2O_2/Vc and CO_2/Ar, and this process is chemically reversible.

7. pH-responsive behavior of 1 in water

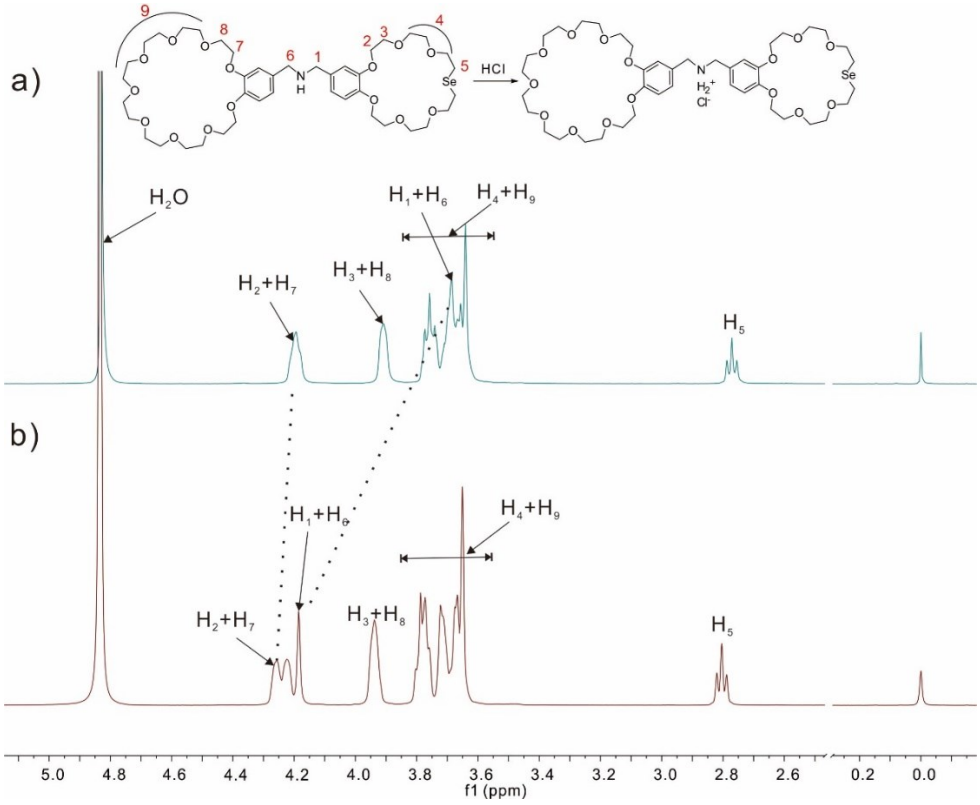

Figure S36. ^{1}H NMR spectra for compound **1** (12 mM) a) before and b) after adding HCl (1 M) to adjust the pH = 4 (D_2O, 400 MHz, 298 K, d_4-trimethylsilyspropionic acid sodium salt as internal standard).

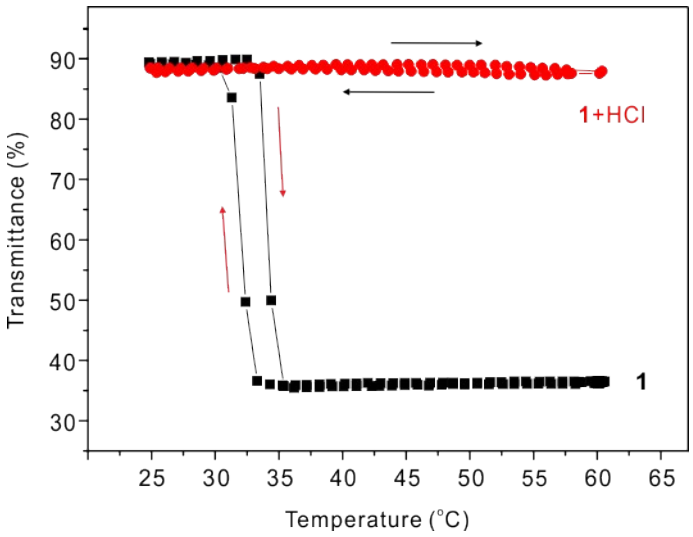

Figure S37. Transmittance as a function of temperature for aqueous solution of **1** and in the presence of HCl (1 M).

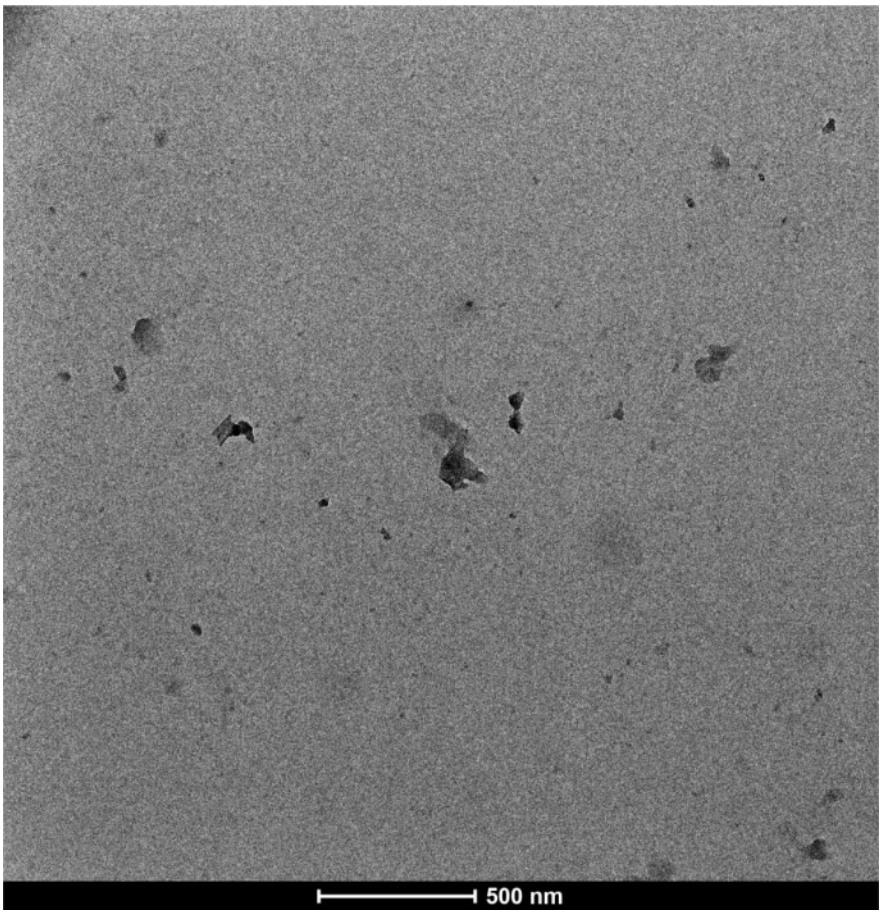

Figure S38. TEM images of aqueous solution of **1** (12 mM) a) after adding HCl (1 M) to adjust its pH = 4.

8. The doxorubicin (DOX) encapsulation experiment of micelles formed by 1

We examine the controlled release of small molecules. The hydrophobic anti-cancer drug, doxorubicin (DOX), was used as the model cargo. After uploading with DOX, the TEM images showed that the micelles **1** deformed (Fig. S20, ESI†). In the absence of external stimuli, DOX only showed o than 3% release within 45 h.

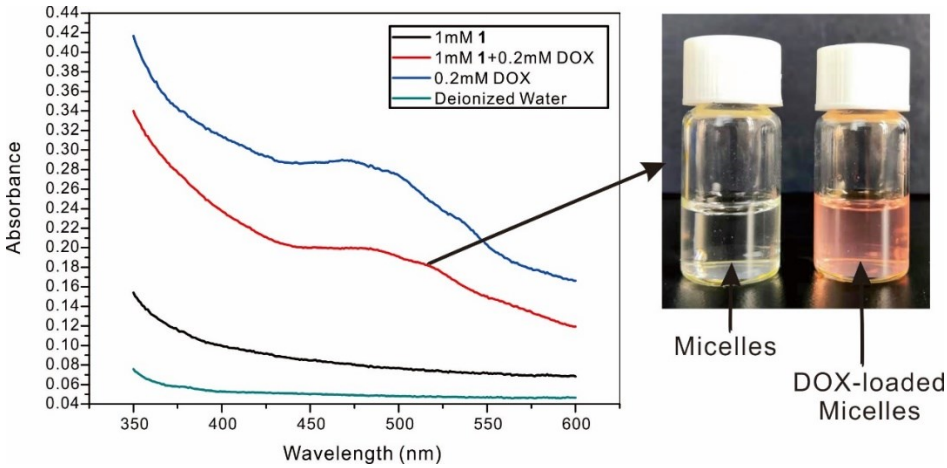

Figure S39. UV/Vis absorption spectra of DOX-loaded micelles, DOX and unloaded micelles in water and water. Inset: color change of DOX-loaded micelles (right) compared with unloaded one (left).

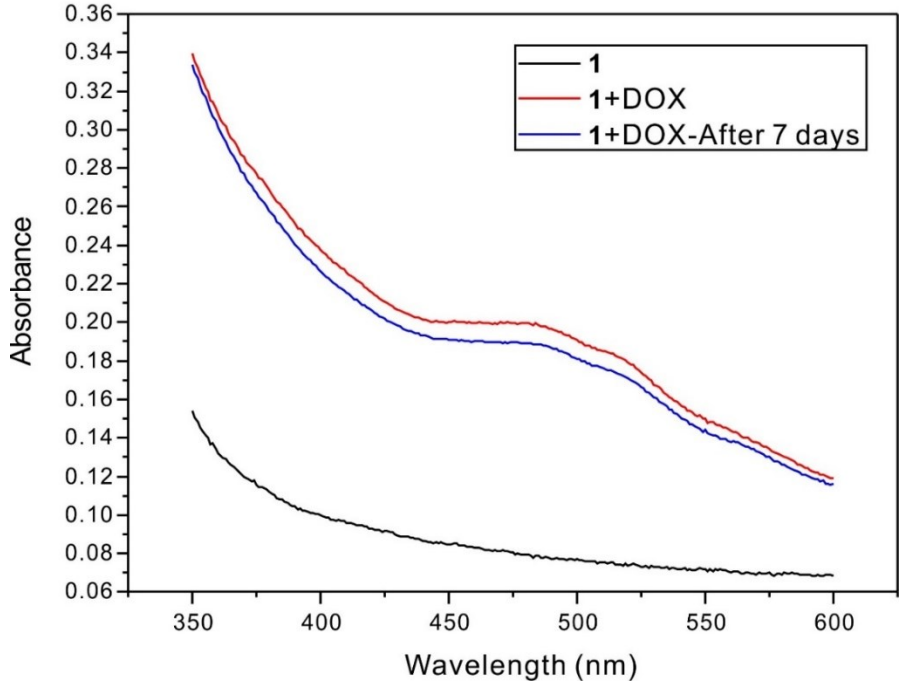

Figure S40. Changes in UV/Vis absorption spectra of DOX-loaded micelles in water with time. [**1**] = 1 mM, [DOX] = 0.2 mM.

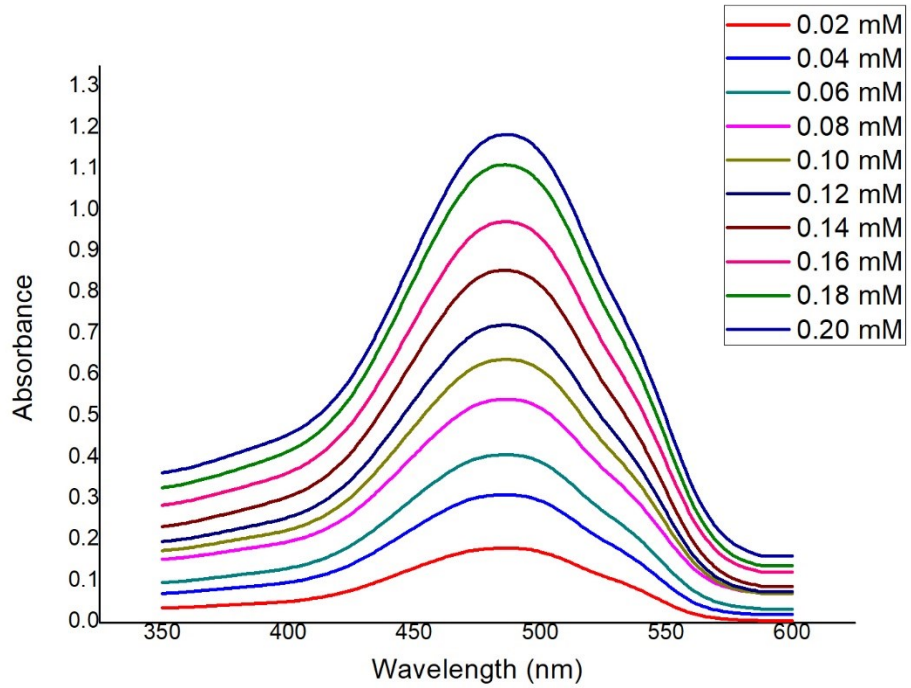

Figure S41. Changes in UV/Vis absorption spectra of DOX with different concentrations in water.

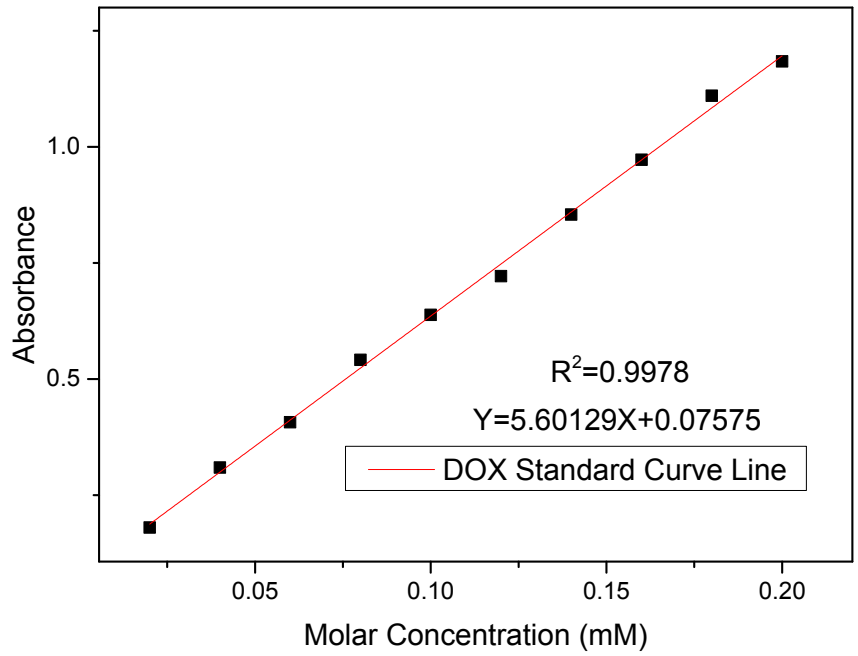

Figure S42. DOX standard curve line determined by the Changes in UV/Vis absorption spectra of DOX with different concentrations in water.

9. Reference

S1 Z. Qi, P. Malo de Molina, W. Jiang, Q. Wang, K. Nowosinski, A. Schulz, M. Gradzielski and C. A. Schalley, *Chem. Sci.*, 2012, **3**, 2073.

S2 L. Jin, B. Li, Z. Cui, J. Shang, Y. Wang, C. Shao, T. Pan, Y. Ge and Z. Qi, *J. Phys. Chem. B*, 2019, **123**, 9692.

S3 E. C. Dreaden, B. E. Gryder, L. A. Austin, B. A. Tene Defo, S. C. Hayden, M. Pi, L. D. Quarles, A. K. Qyelere and M. A. El-Sayed. *Bioconjugate Chem.,* 2012, **23**, 1507.

S4 Q. Zhang, Z. Gao, F. Xu, S. Tai, X. Liu, S. Mo, and F. Niu. *Langmuir,* **2012**, *28*, 11979.